PHYSICAL REVIEW D **72,** 113003 (2005)

Radiative two-pion decay of the tau lepton

A. Flores-Tlalpa* and G. López Castro†

Departamento de Física, Cinvestav, Apartado Postal 14-740, 07000 México, D.F. México

G. Toledo Sánchez‡

Instituto de Física, UNAM, Apartado Postal 20-364, 01000 México, D.F. México

(Received 15 November 2005; published 28 December 2005)

We consider the bremsstrahlung and model-dependent contributions to the radiative decay $\tau^- \to \pi^-\pi^0\nu_\tau\gamma$ in the context of a meson dominance model. We focus on several observables related to this decay, including the branching ratio and the photon and di-pion spectra. Particular attention is paid to the sensitivity of different observables upon the effects of model-dependent contributions and of the magnetic dipole moment of the $\rho^-(770)$ vector meson. Important numerical differences are found with respect to results obtained in the framework of chiral perturbation theory.

DOI: 10.1103/PhysRevD.72.113003 PACS numbers: 13.35.Dx, 12.40.Vv, 13.40.Ks, 14.40.Cs

I. INTRODUCTION

Semileptonic tau lepton decays are a rich source of information about the properties of hadronic resonances below the tau lepton mass scale. They provide a clean environment to study the properties of charged $\rho(770)$ and $a_1(1260)$ resonances which otherwise would be produced only through purely hadronic processes. The interplay of strong, weak, and electromagnetic interactions in such processes offers an interesting place to test models for these interactions at low energies and to extract information about fundamental parameters of the standard model [1].

In this paper we are interested in the study of the radiative $\tau^- \to \pi^-\pi^0\nu_\tau\gamma$ decay, a process that involves simultaneously the three fundamental interactions at the lowest order. This decay channel has been studied previously in Refs. [2,3] within different models and with different purposes. As is well known, the corresponding nonradiative $\tau^- \to \pi^-\pi^0\nu_\tau$ decay is dominated by the production of the $\rho^-(770)$ vector meson; thus, the emission of a single photon from this process is expected to carry information about the ρ^--meson magnetic dipole moment [2]. A meaningful extraction of this property from data is possible only with a full account of the model-dependent contributions to the radiative decay, which was not included in Ref. [2]. In this paper we pursue this study and consider the complete calculation of the radiative amplitude using a phenomenological model that includes all possible intermediate hadronic states.

A different approach is followed in Ref. [3], where the radiative amplitudes were calculated in the framework of chiral perturbation theory and including resonances in the relevant kinematical regions. The interest of Ref. [3] was focused on the relationship between the di-pion tau decay data and its leading hadronic contribution to the anomalous magnetic moment of the muon a_μ [4]. As is known, present experimental information on $\tau \to \pi\pi\nu$ decays are photon inclusive measurements [1]. Thus, removing radiative effects from the measured di-pion mass distribution in such decays is important to predict the leading order hadronic vacuum polarization contribution to a_μ. A comparison of the two-pion mode in tau decays and e^+e^- annihilations provides a sensitive test of the conserved vector-current constraint hypothesis. At present, the prediction of $a_\mu^{\rm had}$ based on $\tau \to \pi\pi\nu$ data seems to exceed by more than 2 standard deviations the corresponding prediction based on e^+e^- data [1], even after the known sources of isospin breaking corrections are removed [3,5,6]. Since the production of high energy photons in $\tau^- \to \pi^-\pi^0\nu\gamma$ decays is driven by the model-dependent contributions, a good account of the model-dependent effects is again mandatory.

This paper is organized as follows: In Sec. II we describe the necessary one-loop modifications of the propagator and electromagnetic vertex of the unstable ρ^- vector meson to achieve a gauge-invariant amplitude for the model-independent contributions; in Sec. III we describe the form of the amplitude for the nonradiative τ lepton decay and fix the parameters involved in our approximation; in Sec. IV we focus on the different contributions to the radiative decay amplitude and check their gauge invariance requirements; in Sec. V we fix the coupling constants involved in the model-independent contributions and compute the different observables associated to the radiative two-pion τ lepton decays; our conclusions are summarized in Sec. VI; and the Appendix is devoted to discuss the kinematics associated with the four-body decay.

II. GAUGE INVARIANCE AND UNSTABLE PARTICLES IN RADIATIVE PROCESSES

The physical amplitudes of radiative processes ($\mathcal{M} = \epsilon^\mu \mathcal{M}_\mu$, ϵ being the photon polarization four-vector) have

*Electronic address: afflores@fis.cinvestav.mx
†Electronic address: glopez@fis.cinvestav.mx
‡Electronic address: toledo@fisica.unam.mx

to satisfy the electromagnetic gauge invariance condition $k^\mu \mathcal{M}_\mu = 0$, where k is the photon four-momentum. As it has been discussed elsewhere [7], when charged unstable particles are produced as intermediate states of a physical process some care must be taken to make compatible the unstable character of the resonance with the gauge invariance condition. One of the proposals to deal with this problem is the so-called *fermion loop-scheme* (*fls*) for gauge bosons [8]. According to the *fls*, only the fermion contributions in loop corrections to the propagator and electromagnetic vertex of gauge bosons have to be included to render gauge invariant the resonant amplitudes [8].

In the case of hadronic resonances such as the ρ^- meson, it has been suggested that an analogous *boson loop-scheme* (*bls*) [2] can be used to avoid such potential gauge pathologies. It has been shown [2,8] that when particles in loop corrections are massless, the corresponding dressed Green functions obtained in the *fls* and *bls* are the same as the ones obtained using the complex-mass prescription $M_0^2 \to M^2 - iM\Gamma$ (M and Γ are the mass and decay width of the resonance) in the bare Green functions. This prescription has been successfully used [9] to describe experimental data of the elastic and radiative $\pi^+ p$ scattering to extract the mass, width, and magnetic moment of the Δ^{++} baryon resonance.

According to the *boson loop-scheme*, one has to include the absorptive parts of the one-loop corrections to the electromagnetic vertex and the propagator of the resonance in order to satisfy electromagnetic gauge invariance [2]. In the case of a ρ^- vector meson of mass m_ρ and four-momentum q, the one-loop absorptive corrections arising from $\pi^-\pi^0$ meson loops[1] gives the resonant propagator [2]:

$$D_{\rho^-}^{\mu\nu}(q) = -i\frac{g^{\mu\nu} - \frac{q^\mu q^\nu}{m_\rho^2}(1 + i\frac{\Gamma_\rho(q^2)}{\sqrt{q^2}})}{q^2 - m_\rho^2 + i\sqrt{q^2}\Gamma_\rho(q^2)}, \tag{1}$$

where we have defined the energy-dependent width (in the limit of isospin symmetry $m_{\pi^-} = m_{\pi^0} = m_\pi$) as follows:

$$\Gamma_\rho(q^2) = \frac{g_{\rho\pi\pi}^2}{48\pi q^2}(q^2 - 4m_\pi^2)^{3/2}\theta(s - 4m_\pi^2),$$

with $g_{\rho\pi\pi}$ the $\rho\pi\pi$ coupling constant (its value is discussed below).

The one-loop absorptive corrections to the electromagnetic vertex (using the convention $\rho^{-\alpha}(p) \to \rho^{-\beta}(p')\gamma^\delta(k)$ for Lorentz indices and four-momenta) gives the following result [2]:

$$ie\Gamma^{\alpha\beta\delta} = ie(\Gamma_0^{\alpha\beta\delta} + \Gamma_1^{\alpha\beta\delta}), \tag{2}$$

where

$$\Gamma_0^{\alpha\beta\delta} = (p + p')^\alpha g^{\beta\delta} + (k^\beta g^{\alpha\delta} - k^\delta g^{\alpha\beta})\beta(0) - p^\beta g^{\alpha\delta} - p'^\delta g^{\alpha\beta}, \tag{3}$$

is the electromagnetic vertex at the tree-level, and $\beta(0)$ the value of the magnetic dipole moment of the $\rho^-(770)$ meson in units of $e/2m_\rho$ ($\beta(0) = 2$ corresponds to the normal or canonical value of the magnetic dipole moment; typical values of $\beta(0)$ computed in quark models lies in the interval $1.8 \leq \beta(0) \leq 3.0$ [10]). The absorptive part of the $\pi^-\pi^0$ one-loop correction to the electromagnetic vertex of the ρ^- has been computed in Ref. [2] using cutting rules. Its explicit form in the limit of isospin symmetry is given by

$$\begin{aligned}\Gamma_1^{\alpha\beta\delta} = \frac{ig_{\rho\pi\pi}^2}{16\pi(p^2 - p'^2)}\{&A(p^2)p^\alpha T^{\beta\delta}(p) \\ &- A(p'^2)p'^\alpha T^{\beta\delta}(p') + B(p^2)F^{\alpha\beta}(p)k^\delta \\ &+ B(p'^2)F^{\alpha\delta}(p')k^\beta + [A(p^2) + B(p^2)] \\ &\times [F^{\alpha\beta}(p)F^{\eta\delta}(p) + F^{\alpha\delta}(p)F^{\eta\beta}(p)]p_\eta \\ &- [A(p'^2) + B(p'^2)][F^{\alpha\beta}(p')F^{\eta\delta}(p') \\ &+ F^{\alpha\delta}(p')F^{\eta\beta}(p')]p'_\eta\},\end{aligned} \tag{4}$$

where

$$\begin{aligned}B(q) &= 2m_\pi^2 \ln\left|\frac{q^2 + (q^4 - 4m_\pi^2 q^2)^{1/2}}{q^2 - (q^4 - 4m_\pi^2 q^2)^{1/2}}\right| \\ &\quad - (q^4 - 4m_\pi^2 q^2)^{1/2}, \\ A(q^2) &= \frac{2(q^4 - 4m_\pi^2 q^2)^{3/2}}{3q^4}, \\ F^{\mu\nu}(q) &= g^{\mu\nu} - \frac{q^\mu k^\nu}{q\cdot k}, \qquad T^{\mu\nu}(q) = g^{\mu\nu} - \frac{q^\mu q^\nu}{q^2}.\end{aligned} \tag{5}$$

Since the above Green functions satisfy the Ward identity [2] $k^\alpha\Gamma_{\alpha\beta\delta} = [iD_{\beta\delta}(p)]^{-1} - [iD_{\beta\delta}(p')]^{-1}$, the radiative amplitudes involving such vertices and propagators is automatically gauge invariant. We will use this prescription in computing the radiative amplitude of $\tau^- \to \pi^-\pi^0\nu_\tau\gamma$ decay; as it will be discussed below, the model-independent contribution to this process involves the production and decay of an intermediate $\rho^-(770)$ vector meson.

III. NONRADIATIVE TWO-PION DECAY

In this section we focus on the meson dominance model for the nonradiative $\tau^-(P) \to \pi^-(Q)\pi^0(Q')\nu_\tau(P')$ decay, where the particles four-momenta are indicated within parenthesis. Our phenomenological model is based on the quantum-mechanical requirement of unitarity, according to which all possible intermediate states that are allowed to contribute given their quantum numbers have to be in-

[1] The contribution of loops with K^-K^0 mesons can be included in a similar way, but we neglect its small contribution in this paper.

cluded (see Fig. 1). In practice, only a few low-lying meson states are sufficient to describe experimental data. As it can be verified below, this model reproduces the Kühn and Santamaria [11] parametrization of the vector form factor which contains the sum of the $\rho^-(770)$ and of its higher excitations.

In the limit of the isospin symmetry, the amplitude for this decay can be written in terms of a single vector form factor:

$$\mathcal{M}_0 = \frac{G_F V_{ud}}{\sqrt{2}} l^\mu (Q - Q')_\mu f_+(\tilde{t}), \tag{6}$$

where G_F is the Fermi coupling constant, $l^\mu = \bar{u}(P')\gamma^\mu(1-\gamma_5)u(P)$ denotes the leptonic current, $\tilde{t} = (Q+Q')^2$ is the square of the momentum transfer and V_{ud} is the Cabibbo-Kobayashi-Maskawa mixing matrix element.

For the purposes of illustrating how the model works, we will assume that the amplitude is dominated by the exchange of two intermediate resonances: the $\rho^-(770)$ and the $\rho'^-(1450)$ vector mesons as shown in Fig. 1. Applying the Feynman rules to the diagram of Fig. 1 and using the vector-meson propagator given in Eq. (1) we can obtain the following expression for the form factor:

$$\begin{aligned} f_+(\tilde{t}) &= \frac{g_\rho g_{\rho\pi\pi}}{m_\rho^2 - \tilde{t} - i\sqrt{\tilde{t}}\Gamma_\rho(\tilde{t})} + \frac{g_{\rho'} g_{\rho'\pi\pi}}{m_{\rho'}^2 - \tilde{t} - i m_{\rho'}\Gamma_{\rho'}} \\ &= \frac{\sqrt{2}}{1+\sigma}\left\{\frac{m_\rho^2}{m_\rho^2 - \tilde{t} - i\sqrt{\tilde{t}}\Gamma_\rho(\tilde{t})}\right. \\ &\quad \left. + \sigma \frac{m_{\rho'}^2}{m_{\rho'}^2 - \tilde{t} - i m_{\rho'}\Gamma_{\rho'}}\right\}, \end{aligned} \tag{7}$$

where $g_\rho (g_{\rho'})$ denotes the weak coupling of the $\rho(770)(\rho'(1450))$ vector meson (we neglect the energy dependence of the decay width of the ρ' meson).

The expression for the form factor in the second line of Eq. (7), which coincides with the model of Ref. [11], follows from imposing the normalization condition $f_+(\tilde{t} = 0) = \sqrt{2}$ and from the definition of the parameter $\sigma \equiv (m_\rho^2 g_{\rho'} g_{\rho'\pi\pi})/(m_{\rho'}^2 g_\rho g_{\rho\pi\pi})$. Using the experimental data on the ρ and ρ' decays [12] (we take $\Gamma(\rho' \to e^+e^-) = 1.48$ keV, $\Gamma(\rho' \to \pi^+\pi^-) = 26.9$ MeV, which we have estimated from relevant inputs in Ref. [12]), we can obtain the following estimate for the relative strengths of these vector-meson contributions in Eq. (7):

$$\sigma = \sqrt{\frac{m_{\rho'}\Gamma(\rho' \to e^+e^-)\Gamma(\rho' \to \pi\pi)(m_\rho^2 - 4m_\pi^2)^{3/2}}{m_\rho\Gamma(\rho \to e^+e^-)\Gamma(\rho \to \pi\pi)(m_{\rho'}^2 - 4m_\pi^2)^{3/2}}} \approx 0.102. \tag{8}$$

This estimate is very close to the experimental value ($|\sigma^{\exp}| = 0.120 \pm 0.008$) reported in Ref. [13] [see also our fit discussed after Eq. (10)]. This agreement renders confidence on the meson dominance model for the radiative decays to be discussed in this paper, and, in particular, about the values of the coupling constants extracted from other independent measured processes (see Sec. V).

In order to provide a comparison with the results obtained for radiative τ lepton decays in chiral perturbation theory [3], hereafter we will restrict to the model with a single resonance, namely, the $\rho(770)$. In order to fix the parameters of this model, we have fitted the data of Ref. [14] for the pion form factor below $\sqrt{\tilde{t}} \approx 1.1$ GeV and have found that the approximation of using only one resonance gives a good description of data with the following central values for the resonance parameters:

$$m_\rho = 776.66 \text{ MeV}, \qquad g_{\rho\pi\pi} = 5.488. \tag{9}$$

Using these values for the resonance parameters, we obtain the following result for the nonradiative branching fraction:

$$B(\tau^- \to \pi^-\pi^0\nu_\tau) = 20.75\%. \tag{10}$$

Clearly, our simple model underestimates the experimental value whose present world average is $B^{\exp}(\tau^- \to \pi^-\pi^0\nu) = (25.47 \pm 0.13)\%$ [1]. This discrepancy can be attributed mainly to the fact that we have neglected the contribution of the $\rho(1450)$ resonance which affects the higher energy tail of the hadronic spectrum (indeed, if we repeat the fit to data of Ref. [14] using the two vector resonance model in Eq. (7), fixing the mass and width of the ρ' to their PDG values [12] and assuming that σ is real,

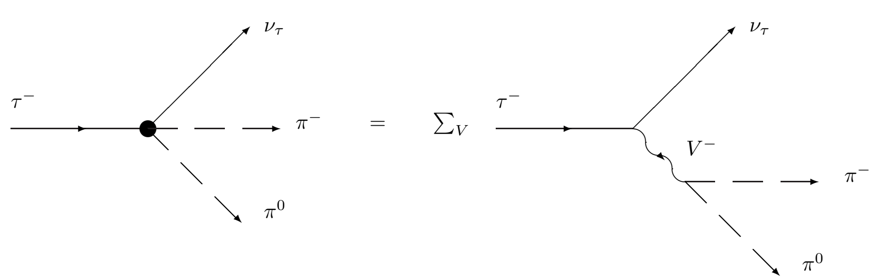

FIG. 1. Meson dominance model of the nonradiative decay $\tau^- \to \pi^-\pi^0\nu_\tau$.

we get $m_\rho = 775.80$ MeV, $g_{\rho\pi\pi} = 5.867$, and $\sigma = -0.12$; this in turn leads to $B(\tau^- \to \pi^-\pi^0\nu_\tau) = 23.27\%$, which is closer to the experimental value).

It is worth mentioning that in Ref. [3], the authors have used the following form factor:

$$f_+^{\rm GP}(\tilde{t}) = \frac{\sqrt{2}m_\rho^2}{m_\rho^2 - \tilde{t} - im_\rho\Gamma_\rho^{\rm GP}(\tilde{t})}\exp[2\tilde{H}_{\pi\pi}(\tilde{t}) + \tilde{H}_{K\bar{K}}(\tilde{t})], \tag{11}$$

which is obtained [15] by matching the prediction of chiral perturbation theory at $O(p^4)$ with the contribution of the $\rho(770)$ in the resonance region. The expressions of $\Gamma_\rho^{\rm GP}(\tilde{t})$ (which differs from our decay rate given in Sec. II) and of the loops functions $\tilde{H}_{PP'}(\tilde{t})$ can be found in Refs. [3,15]. As in our model, the form factor in Eq. (11) gives a good description of experimental data for the two-pion spectra in the region below $\sqrt{\tilde{t}} = 1.1$ GeV.

The branching ratio for the nonradiative decay that is obtained using the form factor in Eq. (11) also underestimates the experimental value since:

$$B(\tau \to \pi\pi\nu) = 21.19\%. \tag{12}$$

This low branching ratio reflects again the fact that the form factor in Eq. (11) underestimates experimental data of the pion form factor for large values of $\tilde{t}$. One possibility to account for this discrepancy in the predictions of our model is to normalize our results for radiative decays in terms of the nonradiative rate. However, for the purposes of comparing our results with those of Ref. [3] we keep the one-resonance model with the ρ^- contribution in the evaluation of the model-independent radiative amplitudes.

IV. RADIATIVE DECAY MODE

The Feynman diagrams that contribute to the radiative $\tau^-(p) \to \pi^-(p_-)\pi^0(p_0)\nu_\tau(q)\gamma(k,\epsilon)$ decay in our meson dominance model are shown in Fig. 2. The particles four-momenta are indicated within parenthesis, with $k(\epsilon)$ denoting the momentum and polarization four-vectors of the photon.

The decay amplitude has the following generic expansion in powers of the photon energy E_γ [16]:

$$\mathcal{M} = \frac{\mathcal{A}}{E_\gamma} + \mathcal{B}E_\gamma^0 + CE_\gamma + \cdots, \tag{13}$$

where the ellipsis denotes the terms of higher order in E_γ. As we will see below, the terms of order up to E_γ^0 (Low's amplitude) contains only model-independent contributions, while the terms starting at order E_γ arise from model-dependent contributions and from the magnetic dipole [$\beta(0)$] and electric quadrupole moments (Q_ρ) of the ρ^- meson (in this paper we do not consider the possible effects of Q_ρ). In the following we consider the different contributions in more detail.

A. Model-independent contributions

The model-independent contributions [Fig. 2(a)–2(d)] are obtained by attaching the photon to all the charged lines and vertices with derivate couplings in the nonradiative Feynman diagram. This set of diagrams leads to a gauge-invariant amplitude. In our model, gauge invariance is guaranteed owing to the Ward identity satisfied by the electromagnetic coupling and propagator of the ρ^- introduced in Sec. II. In other words, we do not need to *impose* gauge invariance to the model-independent amplitude due to the finite width effects of the ρ^- vector meson. Just for a later comparison, let us mention that the effects of the ρ^--meson magnetic moment $\beta(0)$, a gauge-invariant term by itself, can not be obtained by imposing gauge invariance to the sum of amplitudes obtained from diagrams (*a, c, d*) in Fig. 2.

Using the Feynman rules corresponding to the vertices and propagators in diagrams (a-d) from Fig. 2, we obtain the following amplitudes:

$$\mathcal{M}_a = eG_FV_{ud}\frac{ig_\rho g_{\rho\pi\pi}}{\sqrt{2}}\frac{(p_- - p_0)_\kappa D_{\rho^-}^{\beta\kappa}(p_- + p_0)}{2p\cdot k} \times \bar{u}(q)\gamma_\beta(1-\gamma_5)(\not{p} - \not{k} + m_\tau)\not{\epsilon}^* u(p), \tag{14}$$

$$\mathcal{M}_b = eG_FV_{ud}\frac{g_\rho g_{\rho\pi\pi}}{\sqrt{2}}(p_- - p_0)_\nu D_{\rho^-}^{\mu\nu}(p_- + p_0) \times \Gamma_{\kappa\eta\mu}D_{\rho^-}^{\delta\eta}(p-q)\epsilon^{*\kappa}l_\delta, \tag{15}$$

$$\mathcal{M}_c = -eG_FV_{ud}\frac{ig_\rho g_{\rho\pi\pi}}{\sqrt{2}}\frac{p_-\cdot\epsilon^*}{p_-\cdot k} \times (k + p_- - p_0)_\eta D_{\rho^-}^{\delta\eta}(p-q)l_\delta, \tag{16}$$

$$\mathcal{M}_d = eG_FV_{ud}\frac{ig_\rho g_{\rho\pi\pi}}{\sqrt{2}}\epsilon_\eta^* D_{\rho^-}^{\delta\eta}(p-q)l_\delta. \tag{17}$$

Owing to the Ward identity given in Sec. II, it is easy to verify that the model-independent amplitude $\mathcal{M}_{\rm MI} = \mathcal{M}_a + \mathcal{M}_b + \mathcal{M}_c + \mathcal{M}_d$ is gauge-invariant, namely $\mathcal{M}_{\rm MI}(\epsilon^* \to k) = 0$. The amplitude $\mathcal{M}_{\rm MI}$ differs from the corresponding model-independent amplitude of Ref. [3] in terms of order k and due to the effects of the magnetic dipole moment of the ρ^- meson. As we will see later, the effects of $\beta(0)$ are negligible in the integrated observables of this radiative decay. However, as it was discussed elsewhere [2,17], its effects can be enhanced with a special choice of the kinematics (see Sec. V D).

Just to end this section, we provide the Low's amplitude obtained from Eqs. (14)–(17) after expanding the amplitude $\mathcal{M}_{\rm MI}$ around the soft-photon limit [the form factor $f_+(t)$ used here corresponds to the expression in Eq. (7) when $\sigma = 0$]:

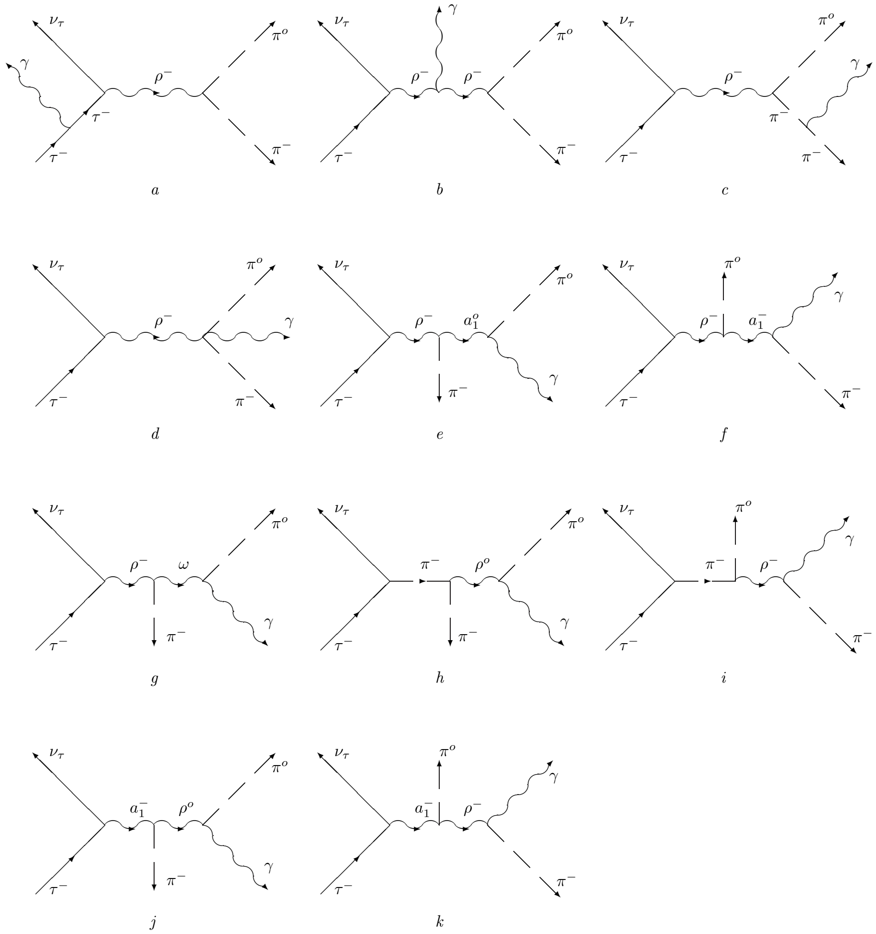

FIG. 2. Feynman diagrams of the model-independent (a-d) and model-dependent (e-k) contributions to $\tau^- \to \pi^- \pi^0 \nu_\tau \gamma$ decays.

$$\begin{aligned}\mathcal{M}_{\text{Low}} = \frac{eG_F V_{ud}}{\sqrt{2}} \bigg\{ & f_+(t)\bigg(\frac{\epsilon^* \cdot p_-}{k \cdot p_-} - \frac{\epsilon^* \cdot p}{k \cdot p}\bigg)(p_- - p_0)^\nu l_\nu \\ & + \frac{f_+(t)}{2k \cdot p} \bar{u}(q)(\not{p}_- - \not{p}_0)\not{k}\not{\epsilon}^*(1 - \gamma_5)u(p) \\ & - f_+(t)\bigg(\epsilon^{*\nu} - \frac{\epsilon^* \cdot p_-}{k \cdot p_-} k^\nu\bigg) l_\nu + 2\frac{\mathrm{d}f_+(t)}{\mathrm{d}t} \\ & \times \bigg(\frac{\epsilon^* \cdot p_-}{k \cdot p_-} k \cdot p_0 - \epsilon^* \cdot p_0\bigg)(p_- - p_0)^\nu l_\nu \bigg\}. \end{aligned} \tag{18}$$

As it can be easily checked, this amplitude coincides with the one obtained in Ref. [3]. As is dictated by Low's soft-photon theorem [16], the amplitude depends only on the nonradiative amplitude and on the static electromagnetic properties of the external particles.

B. Model-dependent contributions

The model-dependent contributions that appear within our meson dominance model are shown in Figs. 2 (e-k). The diagrams (e-g) contribute to an effective vector hadronic current, while the diagrams (h-k) give rise to an effective axial current. We can write these vector and axial model-dependent contributions to the amplitude as follows:

$$\mathcal{M}_V = eG_F V_{ud} \epsilon^{*\mu} [V^e_{\mu\delta} + V^f_{\mu\delta} + V^g_{\mu\delta}] l^\delta, \tag{19}$$

$$\mathcal{M}_A = eG_F V_{ud} \epsilon^{*\mu} [A^h_{\mu\delta} + A^i_{\mu\delta} + A^j_{\mu\delta} + A^k_{\mu\delta}] l^\delta. \tag{20}$$

The explicit expressions for the vector and axial terms of the hadronic vertex are the following:

$$\begin{aligned} V^e_{\mu\delta} = \frac{g_\rho g_{\rho a_1 \pi} g_{\gamma a_1 \pi}}{\sqrt{2} e} & [k \cdot p_0 g_{\lambda\mu} - k_\lambda p_{0\mu}] D^{\kappa\lambda}_{a_1}(k + p_0) \\ & \times [(k + p_0) \cdot (p - q) g_{\eta\kappa} \\ & - (k + p_0)_\eta (p - q)_\kappa] D_{\rho^- \delta}{}^\eta (p - q), \end{aligned} \tag{21}$$

$$\begin{aligned} V^f_{\mu\delta} = \frac{g_\rho g_{\rho a_1 \pi} g_{\gamma a_1 \pi}}{\sqrt{2} e} & [k \cdot p_- g_{\lambda\mu} - k_\lambda p_{-\mu}] D^{\kappa\lambda}_{a_1}(k + p_-) \\ & \times [(k + p_-) \cdot (p - q) g_{\eta\kappa} - (k + p_-)_\eta (p - q)_\kappa] \\ & \times D_{\rho^- \delta}{}^\eta (p - q), \end{aligned} \tag{22}$$

$$V^g_{\mu\delta} = \frac{g_\rho g_{\rho\omega\pi} g_{\gamma\omega\pi}}{\sqrt{2}e} \epsilon_{\lambda'\lambda\mu'\mu} p_0{}^{\lambda'} k^{\mu'} D^{\kappa\lambda}_{\omega}(k + p_0) \times \epsilon_{\eta'\eta\kappa'\kappa} p_-{}^{\eta'} (k + p_0)^{\kappa'} D_{\rho^-\delta}{}^{\eta}(p - q), \quad (23)$$

$$A^h_{\mu\delta} = \frac{f_\pi g_{\rho\pi\pi} g_{\rho\pi\gamma}}{\sqrt{2}e[(p-q)^2 - m^2_\pi]} \epsilon_{\eta'\eta\mu'\mu} p_0{}^{\eta'} k^{\mu'} D^{\kappa\eta}_{\rho^-}(k + p_0) \times (p - q + p_-)_\kappa (p - q)_\delta, \quad (24)$$

$$A^i_{\mu\delta} = \frac{f_\pi g_{\rho\pi\pi} g_{\rho\pi\gamma}}{\sqrt{2}e[(p-q)^2 - m^2_\pi]} \epsilon_{\eta'\eta\mu'\mu} p_-{}^{\eta'} k^{\mu'} D^{\kappa\eta}_{\rho^-}(k + p_-) \times (p - q + p_0)_\kappa (p - q)_\delta, \quad (25)$$

$$A^j_{\mu\delta} = \frac{i f_{a_1} g_{\rho a_1\pi} g_{\rho\pi\gamma}}{\sqrt{2}e} \epsilon_{\lambda'\lambda\mu'\mu} p_0{}^{\lambda'} k^{\mu'} D^{\kappa\lambda}_{\rho^-}(k + p_0)[(k + p_0) \cdot (p - q) g_{\eta\kappa} - (k + p_0)_\eta (p - q)_\kappa] D_{a_1\delta}{}^{\eta}(p - q), \quad (26)$$

$$A^k_{\mu\delta} = \frac{i f_{a_1} g_{\rho a_1\pi} g_{\rho\pi\gamma}}{\sqrt{2}e} \epsilon_{\lambda'\lambda\mu'\mu} p_-^{\lambda'} k^{\mu'} D^{\kappa\lambda}_{\rho^-}(k + p_-)[(k + p_-) \cdot (p - q) g_{\eta\kappa} - (k + p_-)_\eta (p - q)_\kappa] D_{a_1\delta}{}^{\eta}(p - q). \quad (27)$$

All the couplings constants appearing in the above expressions can be easily identified from the corresponding diagrams in Fig. 2. Their values can be fixed from measured decays of the a_1, π, ρ, and ω mesons and will be provided in the next section. Note that when the vector and axial vector mesons become heavy degrees of freedom, these model-dependent contributions vanish as required by chiral symmetry [3].

As already anticipated, the above amplitudes are of order 1 in the photon four-momentum k. Moreover, they are individually gauge invariant since the conditions $k^\mu V^m_{\mu\delta} = k^\mu A^n_{\mu\delta} = 0$ are satisfied. Of course, the vector and axial amplitudes given above can be decomposed in terms of a basis of four-independent vector and axial tensors as pointed out in Ref. [3].

V. DECAY OBSERVABLES

As it was discussed in the previous section, the decay amplitude of the radiative τ lepton decay depends on a large set of parameters (coupling constants and masses of mesons). The parameters m_{ρ^-}, $g_{\rho\pi\pi}$ entering the model-independent contributions where fixed from a fit to experimental data [14] in the di-pion mass spectrum of the decay $\tau \to \pi\pi\nu$ in the region below 1.1 GeV. Their values were given in Eq. (9) of Sec. III. The other free parameter entering the model-independent amplitude, namely, the magnetic dipole moment $\beta(0)$ of the ρ^- meson, is left as a free parameter in order to study their effects on the different observables of radiative τ decays.

The model-dependent contributions depend mainly on the values of the coupling constants and masses of the vector (ρ, ω), axial a_1 and pseudoscalar π mesons (we assume isospin symmetry for the masses of neutral and charged states). The values of the coupling constants can be obtained from the measured decay rates of these mesons (except for the weak coupling of the a_1 meson whose value is fixed from the Weinberg sum rule $f_{a_1} = g_\rho$ [18]). As it was the case for the nonradiative decay in Sec. III, we expect that these effective couplings will give a good estimate of the correct size for model-dependent effects. Based on the experimental data compiled in Ref. [12], we will use the following central values:

$$g_\rho = 167\,765.48 \text{ MeV}, \quad (28)$$

$$f_\pi = 130.7 \text{ MeV}, \quad (29)$$

$$g_{\rho a_1\pi} = 4.843 \times 10^{-3} \text{ MeV}^{-1}, \quad (30)$$

$$g_{\gamma a_1\pi} = 2.9265 \times 10^{-4} \text{ MeV}^{-1}, \quad (31)$$

$$g_{\rho\omega\pi} = 0.012 \text{ MeV}^{-1}, \quad (32)$$

$$g_{\gamma\omega\pi} = 7.1126 \times 10^{-4} \text{ MeV}^{-1}, \quad (33)$$

$$g_{\rho\pi\gamma} = 2.2092 \times 10^{-4} \text{MeV}^{-1}. \quad (34)$$

Once we have fixed the values of these parameters, we proceed to compute the different observables associated to the radiative τ lepton decay. Using the choice of kinematical variables described in the Appendix, we can write the differential decay rate in terms of the five independent kinematical variables as follows:

$$\mathrm{d}\Gamma = \frac{\beta_{-0}}{2(4\pi)^6 m^2_\tau} \frac{1}{2} \sum_{\text{pols}} |\mathcal{M}|^2 \mathrm{d}x \mathrm{d}t \mathrm{d}E_\gamma \mathrm{d}\cos\theta_{\pi^-} \mathrm{d}\phi_{\pi^-}, \quad (35)$$

where $\beta_{-0} = \sqrt{1 - 4m^2_\pi/t}$ is the magnitude of the pion velocity in the di-pion rest frame. In order to integrate over the relevant kinematical variables we have used the VEGAS [19] integration routine. Next we focus on the results obtained for each one of the computed observables.

A. Branching ratios

In this subsection we compute the predictions of our model for the branching ratios. As it was done in Ref. [3], we distinguish between the *bremsstrahlung* (model-independent) and the *full* (that includes also model-dependent terms) contributions to the decay rate. Since the unpolarized probability is divergent for soft photons, we introduce a cutoff energy $E^{\min}_\gamma$ to regularize the integral. In Fig. 3 we show the branching ratio as a function of $E^{\min}_\gamma$,

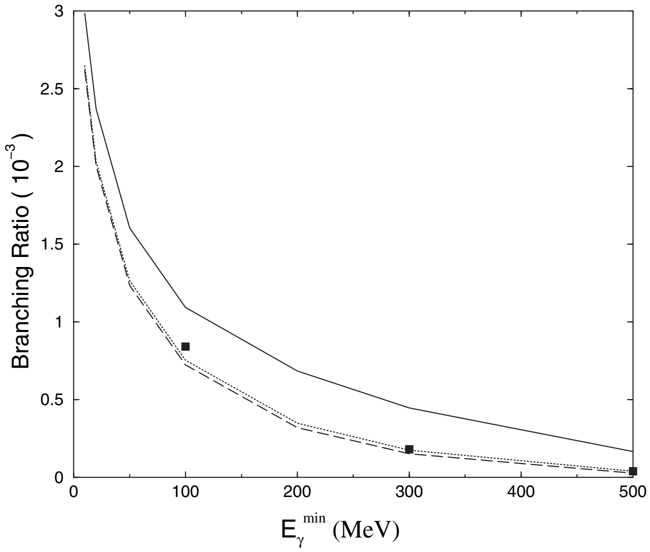

FIG. 3. Branching ratio of $\tau \to \pi^- \pi^0 \nu \gamma$ as a function of the soft-photon cutoff $E_\gamma^{\rm min}$ for $\beta(0) = 2$. The dashed line denotes the model-independent contributions and the solid line the full contributions. The dotted line is obtained by excluding the contribution of the ω meson, diagram 2(g). The points at $E_\gamma = 100$, 200, and 300 MeV correspond to the full contributions of Ref. [3].

for the normal value of the magnetic dipole moment $\beta(0) = 2$. We compare our results with the predictions based on chiral perturbation theory [3] (the three squares in Fig. 3).

We observe that if we exclude the ω meson contribution, diagram in Fig. 2(g), we find a very good agreement with the calculation of Ref. [3]. However, according to the VMD model, the contribution of the $\omega(782)$ vector meson cannot be excluded. This particular model-dependent contribution becomes large due to a particular kinematic accident, namely, the almost degeneracy of the $\rho^- - \omega$ system, and due to the small decay width of the ω meson ($\Gamma_\omega = 8.44$ MeV). This double resonance effect produces an enhancement of the decay amplitude in approximately the same kinematical region. In order to verify this explanation we have increased the mass difference of the $\rho^- \omega$ mesons and/or the width of the ω meson and have found that the large effect of the ω meson is decreased in an important way. We find that for photon cutoff energies of order $E_\gamma^{\rm min} = 200$ MeV, the contribution of the ω meson becomes already twice the value of all other contributions. Therefore, a measurement of the radiative decay branching ratio can help to discriminate among the two models.

The branching ratio is almost insensitive to reasonable variations in the value of the ρ^--meson magnetic dipole moment $\beta(0)$. In Fig. 4 we show the full branching ratio as a function of $E_\gamma^{\rm min}$ for $\beta(0) = 1$, 2, and 3. Thus, it is clear that this observable cannot help to discriminate values of the magnetic dipole moment.

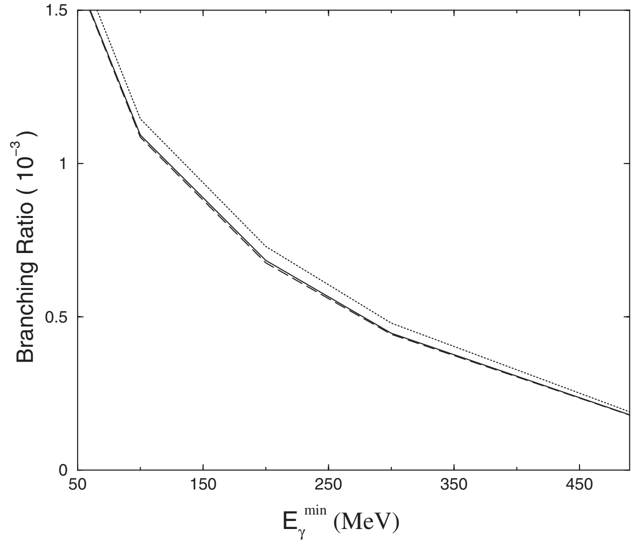

FIG. 4. Branching ratio of $\tau \to \pi^- \pi^0 \nu \gamma$ as a function of the soft-photon cutoff $E_\gamma^{\rm min}$ for $\beta(0) = 1, 2, 3$ (respectively, dashed, solid, and dotted lines). Only the full contributions are plotted in this case.

B. Photon spectrum

The photon spectrum can be obtained after integrating over all the kinematical variables in Eq. (35) except E_γ. This spectrum $d\Gamma/dE_\gamma$ is plotted in Fig. 5 for $\beta(0) = 2$. The effect of the ω meson contribution is particularly important for $E_\gamma \geq 180$ MeV. As in the case of the branching ratio, the photon spectrum is not sensitive to the value of the ρ^- magnetic dipole moment.

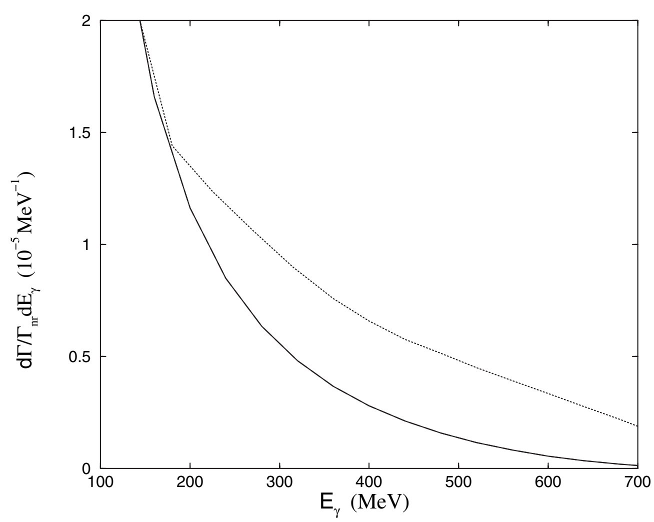

FIG. 5. Photon spectrum in the $\tau \to \pi^- \pi^0 \nu \gamma$ decay. The solid line denotes the model-independent contributions, while the dotted line is used for the full contributions. The dashed line (almost superposed over the solid line) corresponds to the full contribution obtained by excluding Fig. 2(g). The observable is normalized to the nonradiative decay rate.

C. Di-pion invariant mass distribution

Another important observable associated to $\tau^- \to \pi^- \pi^0 \nu\gamma$ is the invariant mass distribution of the di-pion system. In the case of the corresponding nonradiative decay, this spectrum shows explicitly the peaks associated to the production of vector resonances. It is interesting to study how they are modified by the radiation of photons. On another hand, a detailed study of this spectrum in radiative decays is very important in order to remove the hard bremsstrahlung from photon inclusive measurements of $\tau^- \to \pi^- \pi^0 \nu(\gamma)$ decays [1].

In Fig. 6 we plot the combined photon and di-pion invariant mass spectra $d\Gamma/\Gamma_{\rm nr} dE_\gamma dt$ ($\Gamma_{\rm nr}$ is the nonradiative decay rate) by choosing $\beta(0) = 2$. In order to avoid the infrared divergences due to the emission of soft-photons, we plot our results for a finite value of the photon energy E_γ. Once again, we observe that the presence of the ω-meson contribution changes the spectrum in a sizable way in all the region of t. However, the position of the peaks associated to the photon emission off the π^- and the τ^- external lines are not affected. We also plot in Fig. 7 the di-pion invariant mass distribution after integrating the previous result for photons of energy larger than 300 MeV (unfortunately, a quantitative comparison with results of Ref. [3] is not possible since they give their results in arbitrary units). As in the case of the branching ratios and of the photon spectrum studied in previous subsections, the di-pion invariant mass distribution can also help to distinguish between the present model and the one based in chiral perturbation theory [3].

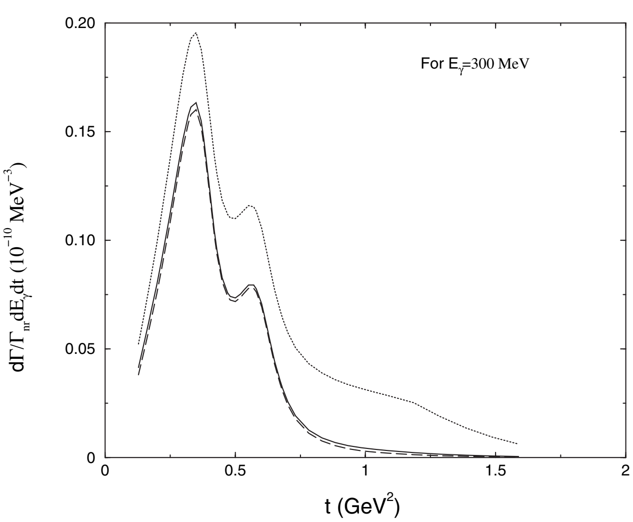

FIG. 6. Distribution in the photon energy and the invariant mass of the di-pion system in $\tau \to \pi^- \pi^0 \nu\gamma$ decays for $E_\gamma = 300$ MeV. The dashed line (dotted line) denotes the model-independent (full) contributions. The solid line is obtained when we exclude the meson ω, diagram in Fig. 2(g). The observable is normalized to the nonradiative rate.

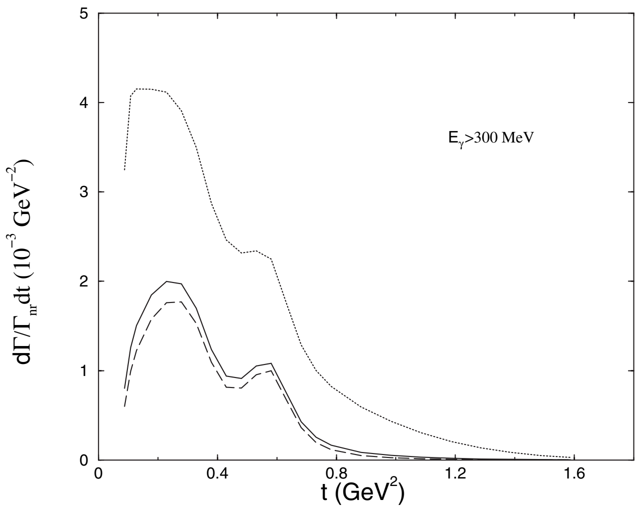

FIG. 7. Di-pion invariant mass distribution in $\tau \to \pi^- \pi^0 \nu\gamma$ decays for photon energies larger than 300 MeV. Description of lines are the same as in Fig. 6. The observable is normalized to the nonradiative rate.

D. Angular and energy photon spectra

Previous studies of radiative decays involving the production and decay of an on-shell charged vector meson [17] have shown that the angular and energy photon spectra are sensitive to the effects of the vector-meson magnetic dipole moment when photons are emitted at small angles. Therefore, we also compute this observable for the case of $\tau \to \pi\pi\nu\gamma$ decays.

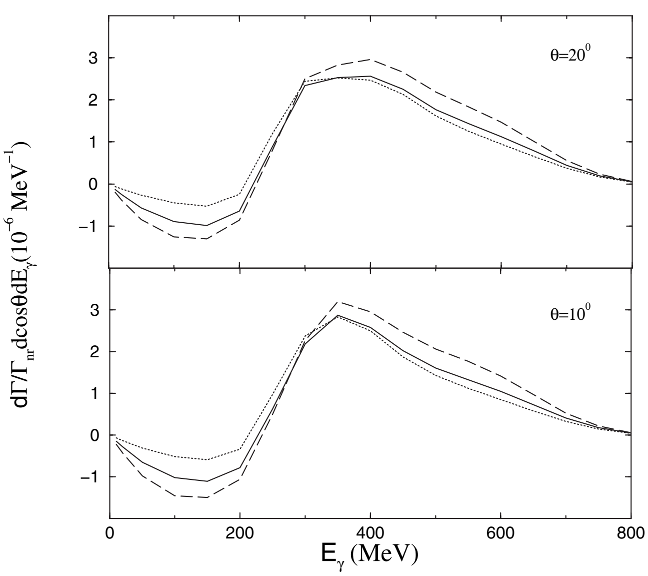

FIG. 8. Reduced angular and energy distribution of photons for three different values of $\beta(0) = 1, 2, 3$ (dotted, solid, and dashed lines) and two different angles of the photon emitted with respect to the π^- three-momentum. The model-independent contributions [for $\beta(0) = 0$] have been subtracted. The observable is normalized to the nonradiative rate.

In Fig. 8 we plot the angular and energy photon spectra $d\Gamma/\Gamma_{\rm nr} d\cos\theta dE_\gamma$ as a function of the photon energy for $\theta = 10°$ and $20°$ (θ is the angle between the photon and the π^- in the τ^- lepton rest frame) and three different values of $\beta(0)$. We have subtracted the (well-known) contribution arising from the pure bremsstrahlung (terms of order k^{-2} in the unpolarized probability) in order to make more visible the effect of $\beta(0)$. We observe that there are some kinematical regions where the sensitivity to $\beta(0)$ is increased and it may eventually help to measure this property.

VI. CONCLUSIONS

In this paper we have considered the radiative two-pion decay of the τ lepton. This decay mode was considered previously in Refs. [2,3]. The new ingredients of the present study include (a) an electromagnetic gauge-invariant description of the model-independent amplitude including intermediate unstable ρ^- mesons and (b) a complete calculation of the model-dependent contributions using a meson dominance model. In the framework of the present model, all the meson states that are allowed to contribute as intermediate particles were included in the calculation of the radiative amplitude. In addition, we study the effects of the ρ^- magnetic dipole moment in the observables of the radiative τ lepton decay.

We have found that in the branching ratio, the photon spectrum and the di-pion invariant mass spectrum of radiative τ lepton decays are sensitive to the model-dependent contributions that include an ω meson intermediate state [Fig. 2(g)]. This contribution produces an important enhancement of these observables with respect to all other contributions arising in the present model. The origin of this enhancement can be traced back to the almost degeneracy of the $\rho - \omega$ masses and due to the small decay width of the ω meson. In the absence of this contribution, our model reproduces the results obtained in the framework of chiral perturbation theory [3]. Since present formulations of the chiral Lagrangian interactions do not include the presence of vector-vector-pseudoscalar vertices, it is natural that the calculation of Ref. [3] has not included the contribution of diagram 2(g). Thus, experimental measurements of the observables studied in this paper can help to assess the approximation involved in different models. Additionally, our calculation confirms that the effects of the model-dependent axial contributions are negligible [3].

The quantitative difference in model-dependent terms may modify the size of the corrections applied to extract the pion form factor from photon inclusive measurements of $\tau \to \pi\pi\nu\gamma$ decays. As is well known [1], this pion form factor seems to be a bit larger than the one obtained from $e^+e^- \to \pi^+\pi^-$ annihilations for squared momentum transfers larger than m_ρ^2, even after known sources of isospin breaking corrections are taken into account. Since this study must consider the effects of virtual radiative corrections, we will consider it elsewhere [20].

The different observables studied in this paper are not sensitive to the effects of the ρ^- magnetic dipole moment. As it was pointed out in Ref. [2] the photon emission off the internal charged ρ meson line [Fig. 2(b)] is expected to carry information about this important property which has not yet been measured. The sensitivity on different values of $\beta(0)$ is slightly increased when we consider the angular and energy photon spectra for almost collinear $\pi^- - \gamma$ particles.[2] Thus, only processes where the charged ρ vector mesons are on their mass shell can offer a better sensitivity to the magnetic dipole moment [17], since the radiation off this electromagnetic moment enters at a lower order in the photon momentum.

ACKNOWLEDGMENTS

The authors acknowledge financial support from Conacyt under Grants Nos. 40473, 41600, and 42026. G. T. acknowledges the Grant No. PAPIIT IN112902-3 from UNAM.

APPENDIX: KINEMATICS

We discuss here the kinematics of the decay $\tau^-(p) \to \pi^-(p_-)\pi^0(p_0)\nu(q)\gamma(k)$; for simplicity we choose the isospin limit $p_0^2 = p_-^2 = m_\pi^2$. The unpolarized squared amplitude for a four-body decay depends upon five independent kinematical variables. We choose this set of independent variables to be (we closely follow Ref. [21]):

$$(x, t, E_\gamma, \cos\theta_{\pi^-}, \phi_{\pi^-}). \tag{A1}$$

The quantity $t = (p_- + p_0)^2 (x = (q + k)^2)$ denotes the squared invariant mass of the two-pion ($\nu\gamma$) system, E_γ is the photon energy in the rest frame of the τ, and (θ_{π^-}, ϕ^-) are the spherical coordinate angles that define the π^- three-momentum in the τ lepton rest frame.

The order of the limits of integration can be conveniently chosen according to the energy or angular distribution that we want to obtain for the observables. We consider four possible choices (after integrating upon the angular variables):

(i) If we integrate successively on E_γ, t, and x, the limits of integration are given by

$$m_\gamma^2 \leq x \leq (m_\tau - 2m_\pi)^2, \tag{A2}$$

$$4m_\pi^2 \leq t \leq (m_\tau - \sqrt{x})^2, \tag{A3}$$

$$\frac{m_\tau^2 + x - t - 2X}{4m_\tau} \leq E_\gamma \leq \frac{m_\tau^2 + x - t + 2X}{4m_\tau}, \tag{A4}$$

[2] As it was concluded in Refs. [17], choosing such small angles helps to suppress radiation off electric charges and make more prominent the radiation off the magnetic dipole moment.

where $2X = \sqrt{\lambda(m_\tau^2, x, t)}$, and m_γ is a cutoff parameter introduced to regularize the infrared divergence.

(ii) If we exchange $x \leftrightarrow t$ in the order of integration of the previous case, their corresponding limits are

$$4m_\pi^2 \le t \le (m_\tau - m_\gamma)^2, \quad (A5)$$

$$m_\gamma^2 \le x \le (m_\tau - \sqrt{t})^2. \quad (A6)$$

(iii) The successive order of integration over t, x, and E_γ, requires the integration region to be defined as

$$m_\gamma \le E_\gamma \le \frac{m_\tau^2 - 4m_\pi^2}{2m_\tau}, \quad (A7)$$

$$0 \le x \le \frac{2E_\gamma(m_\tau^2 - 4m_\pi^2 - 2m_\tau E_\gamma)}{m_\tau - 2E_\tau}, \quad (A8)$$

$$4m_\tau^2 \le t \le \frac{(m_\tau - 2E_\tau)(2m_\tau E_\gamma - x)}{2E_\gamma}. \quad (A9)$$

(iv) Another useful choice is (the order of integration is easily understood):

$$m_\gamma \le E_\gamma \le \frac{m_\tau^2 - 4m_\pi^2}{2m_\tau}, \quad (A10)$$

$$4m_\pi^2 \le t \le m_\tau(m_\tau - 2E_\gamma), \quad (A11)$$

$$0 \le x \le \frac{2E_\gamma(m_\tau^2 - 2m_\tau E_\gamma - t)}{m_\tau - 2E_\gamma}. \quad (A12)$$

Other choices for the order of integrations are also possible. To verify that the different domains of integrations are equivalent, we have performed the numerical integrations using the different domains of integration described above and have verified that the same results are obtained.

[1] For a recent and comprehensive review article see M. Davier, A. Höcker, and Z. Zhang, hep-ph/0507078 and references therein.

[2] G. López Castro and G. Toledo Sanchez, Phys. Rev. D **61**, 033007 (2000).

[3] V. Cirigliano, G. Ecker, and H. Neufeld, J. High Energy Phys. 08 (2002) 002.

[4] R. Alemany, M. Davier, and A. Höcker, Eur. Phys. J. C **2**, 123 (1998).

[5] V. Cirigliano, G. Ecker, and H. Neufeld, Phys. Lett. B **513**, 361 (2001).

[6] S. Ghozzi and F. Jegerlehner, Phys. Lett. B **583**, 222 (2004).

[7] R. G. Stuart, Phys. Lett. B **262**, 113 (1991); **272**, 353 (1991); G. Valencia and S. Willenbrock, Phys. Lett. B **259**, 373 (1991); A. Sirlin, Phys. Rev. Lett. **67**, 2127 (1991); G. López Castro, J. L. Lucio, and J. Pestieau, Mod. Phys. Lett. A **6**, 3679 (1991).

[8] U. Baur and D. Zeppenfeld, Phys. Rev. Lett. **75**, 1002 (1995); E. Argyres *et al.*, Phys. Lett. B **358**, 339 (1995); M. Beuthe, R. González Felipe, G. López Castro, and J. Pestieau, Nucl. Phys. **B498**, 55 (1997); W. Beenakker *et al.*, Nucl. Phys. **B500**, 255 (1997).

[9] G. López Castro and A. Mariano, Phys. Lett. B **517**, 339 (2001); Nucl. Phys. **A697**, 440 (2002).

[10] T. M. Aliev, I. Kanik, and M. Savci, Phys. Rev. D **68**, 056002 (2003); M. Hecht and B. H. McKellar, Phys. Rev. C **57**, 2638 (1998); A. Samsonov, J. High Energy Phys. 12 (2003) 61; S. J. Brodsky and J. R. Hiller, Phys. Rev. D **46**, 2141 (1992); F. T. Hawes and M. A. Pichowsky, Phys. Rev. C **59**, 1743 (1999); K. L. Mitchell and P. C. Tandy, Phys. Rev. C **55**, 1477 (1997); M. A. Pichowsky and T.-S. Lee, Phys. Rev. D **56**, 1644 (1997); L. L. Frankfurt, T. Federico, and M. I. Strikman, Phys. Rev. C **48**, 2182 (1993); P. L. Chung, F. Coester, B. D. Keister, and W. N. Polizou, Phys. Rev. C **37**, 2000 (1988); L. L. Frankfurt, I. L. Grach, L. A. Kondratyuk, and M. Strikman, Phys. Rev. Lett. **62**, 387 (1989); F. Cardarelli *et al.*, Phys. Lett. B **349**, 393 (1995).

[11] J. H. Kühn and A. Santamaria, Z. Phys. C **48**, 445 (1990).

[12] S. Eidelman *et al.*, Phys. Lett. B **592**, 1 (2004).

[13] S. Schael *et al.* (ALEPH Collaboration), Phys. Rep. **421**, 191 (2005).

[14] R. Barate *et al.* (ALEPH Collaboration), Z. Phys. C **76**, 15 (1997).

[15] F. Guerrero and A. Pich, Phys. Lett. B **412**, 382 (1997); D. Gómez Dumm, A. Pich, and J. Portolés, Phys. Rev. D **62**, 054014 (2000).

[16] F. E. Low, Phys. Rev. **110**, 974 (1958).

[17] G. Toledo Sanchez and G. López Castro, Phys. Rev. D **56**, 4408 (1997); **60**, 053004 (1999); J. Phys. G **27**, 2203 (2001).

[18] L. Okun, *Leptons and Quarks* (North-Holland, Amsterdam, 1982), Chap. 13.

[19] G. P. Lepage, J. Comput. Phys. **27**, 192 (1978).

[20] A. Flores-Tlalpa, F. Flores, G. López Castro, and G. Toledo Sánchez (work in progress).

[21] N. Cabibbo and A. Maksymowicz, Phys. Rev. **137**, B438 (1965); A. Pais and S. B. Treiman, Phys. Rev. **168**, 1858 (1968).